Cardiovascular Engineering and Technology, Vol. 10, No. 1, March 2019 *(© 2018)* pp. 69–79
https://doi.org/10.1007/s13239-018-00398-8

A Valveless Pulsatile Pump for the Treatment of Heart Failure with Preserved Ejection Fraction: A Simulation Study

MARCUS GRANEGGER,[1,3] HITENDU DAVE,[1,3] WALTER KNIRSCH,[2,3] BENTE THAMSEN,[1,3] MARTIN SCHWEIGER,[1,3] and MICHAEL HÜBLER[1,3]

[1]Pediatric Cardiovascular Surgery, Department of Surgery, Pediatric Heart Center, University Children's Hospital Zurich, Zurich, Switzerland; [2]Pediatric Cardiology, Department of Surgery, Pediatric Heart Center, University Children's Hospital Zurich, Zurich, Switzerland; and [3]Children's Research Center, University Children's Hospital Zurich, Zurich, Switzerland

(Received 2 August 2018; accepted 3 December 2018; published online 10 December 2018)

Associate Editors Dr. Ajit P. Yoganathan and Dr. Ulrich Steinseifer oversaw the review of this article.

Abstract

Purpose—Effective treatment of patients with terminal heart failure and preserved ejection fraction (HFpEF) is an unmet medical need. The aim of this study was to investigate a novel valveless pulsatile pump as a therapeutic option for the HFpEF population through comprehensive *in silico* investigations.

Methods—The pump was simulated in a numerical model of the cardiovascular system of four HFpEF phenotypes and compared to a typical case of heart failure with reduced ejection fraction (HFrEF). The proposed pump, which was modeled as being directly connected to the left ventricle, features a single valveless inlet and outlet cannula and is driven in co-pulsation with the left ventricle. We collected hemodynamics for two different pump volumes (30 and 60 mL).

Results—In all HFpEF conditions, the 30 mL pump improved the cardiac output by approximately 1 L/min, increased the mean arterial pressure by $> 11\%$ and lowered the mean left atrial pressure by $> 30\%$. With the larger (60 mL) stroke volume, these hemodynamic improvements were more pronounced. In the HFrEF condition however, these effects were three times less in magnitude.

Conclusions—In this simulation study, the valveless pulsatile device improves hemodynamics in HFpEF patients by increasing the total stroke volume. The hemodynamic benefits are achieved with a small device volume comparable to implantable rotary blood pumps.

Keywords—Mechanical circulatory support (MCS), Heart failure, Ventricular assist devices (VADs), Heart failure with preserved ejection fraction (HFpEF).

Address correspondence to Marcus Granegger, Pediatric Cardiovascular Surgery, Department of Surgery, Pediatric Heart Center, University Children's Hospital Zurich, Zurich, Switzerland. Electronic mail: marcus.granegger@kispi.uzh.ch

INTRODUCTION

50% of all heart failure patients suffer from heart failure with preserved ejection fraction (HFpEF),[15] which is a condition where cardiac function is diminished but the left ventricular ejection fraction (LVEF) is above 50%. A large variety of etiologies and factors contribute to the development of HFpEF (i.e., hypertension, diabetic cardiomyopathies, concentric hypertrophies, infiltrative diseases, etc.), leading to a highly heterogeneous patient population. In a large proportion of these patients, left ventricular dimensions are much smaller compared to patients with heart failure with reduced ejection fraction (HFrEF) and the diastolic ventricular function is usually impaired. Established pharmacological treatment for HFrEF could not replicate the success achieved with the former when used in HFpEF patients.[21]

Mechanical circulatory support (MCS) is being increasingly applied as a therapy for end-stage HFrEF, particularly in patients with ischemic and/or dilated cardiomyopathy, to support an underperforming left and/or right ventricle. In these patients, MCS with rotary blood pumps (RBPs) generally increases long-term survival and improves quality of life.[16] With favorable outcomes of RBP implantation in cases of HFrEF, it would seem feasible that MCS might also be a promising approach for HFpEF patients. However, this disease poses distinct challenges for the use of an RBP: The smaller ventricular dimensions in these patients mean reduced end-systolic and end-diastolic volumes. Consequently, continuous ventricular unloading with a RBP might cause severe suction events around the inflow cannula.[4,25] These limitations for RBP use in HFpEF patients are reflected in liter-

1869-408X/19/0300-0069/0 © 2018 Biomedical Engineering Society

ature by the fact that only anecdotal clinical use of MCS in HFpEF patients has been reported.[26,33] Some HFpEF phenotypes, such as hypertrophic cardiomyopathy, are even considered a contraindication for MCS due to the same reasons.[23] As there are no alternatives for terminal HFpEF patients, an MCS treatment option is highly desirable. To that end, Burkhoff *et al.* suggested use of partial circulatory support with an RBP by decompressing the left atrium and pumping blood into the aorta in order to circumvent the complications of the smaller ventricular cavity.[4] Although RBPs improve survival rates for HFrEF patients, they are associated with a high number of adverse events as manifested by thromboembolic and major bleeding complications.[28,34] In part, these complications are caused by poor hemocompatibility intrinsic to the design of RBPs that includes artificial blood-contacting materials and high shear forces induced by the circumferential velocities of the spinning impeller.

Despite the outperformance of pulsatile MCS devices by continuous-flow RBPs in the adult HFrEF population in terms of durability and stroke-free survival,[31] pulsatile devices may be superior in some aspects of blood trauma[7] and reduce certain adverse events such as gastrointestinal bleeding.[22,31] Omnipresent to all blood-contacting devices, thrombus formation remains an issue also for pulsatile MCS devices and is usually observed close to the inlet and outlet valves, which are necessary in conventional pulsatile devices.[13]

Considering these shortcomings of conventional MCS as therapeutic devices for HFpEF, novel approaches are desired to support terminal HFpEF patients.[30] Due to their unique pathophysiology, HFpEF offers the possibility to exploit other working principles for assist devices, different to those applied in current devices, which are designed for the HFrEF patient population. In fact, while systolic ventricular function varies widely in the HFpEF patients,[29] the end-systolic pressure volume relationship (ESPVR) seems to be rather steep,[3,14,27] similar or even steeper than that in healthy humans.[27] In contrast, the ventricular volume in HFrEF patients is enlarged and the ESPVR is flat. Therefore, boundary conditions for an MCS device envisaged for HFpEF patients are vastly different.

An MCS device that increases the ventricular volume during diastole while also capitalizing on the stiff systolic property of the heart may theoretically improve the stroke volume and, consequently, the hemodynamics in HFpEF patients. This can be realized by a pulsatile displacement pump connected to the ventricle with a single valveless cannula acting as in- and outlet. Synchronized to the heart rate the device would operate in co-pulsation: being filled during diastole and ejecting together with the ventricle in systole (when the aortic valve is open).

The aim of this simulation study was to investigate the efficacy of such a device in different HFpEF phenotypes and compare it to a typical HFrEF condition.

MATERIALS AND METHODS

Hemodynamic Data

Typical hemodynamics of four different HFpEF phenotypes were derived from Burkhoff *et al.*[4] and implemented in a numerical model of the cardiovascular system. These four phenotypes are:

1. Hypertrophic cardiomyopathies with small ventricular chambers indicating diastolic dysfunction (HFpEF I).
2. Infiltrative cardiomyopathies with small ventricular chambers indicating diastolic dysfunction and restrictive physiology (HFpEF II).
3. Non-hypertrophic cardiomyopathies without significant cardiovascular diseases, small to normal ventricular chambers indicating diastolic dysfunction with or without restrictive physiology (HFpEF III).
4. One or more underlying cardiovascular conditions with left ventricular (eccentric or concentric) hypertrophy with EF $>$ 50%, usually hypertension and a chronic volume overload state (HFpEF IV).

In addition, hemodynamic data for typical HFrEF patients before LVAD implantation were derived from Gupta *et al.*[11]

The hemodynamic parameters for the five heart failure groups and reference values of healthy individuals[37] are summarized in Table 1. Missing variables such as the time constant of early ventricular relaxation were adopted from other studies with similar patient populations.[25,38]

Numerical Model of the Cardiovascular System

A numerical model similar to previously reported models[4,6,9,25] was employed to simulate the cardiovascular system of HFpEF and HFrEF patients with a body weight of 70 kg. All heart chambers were modeled having a time varying-elastance with nonlinear end-diastolic/end-systolic pressure–volume relationships (EDPVR/ESPVR) and unidirectional valves with the ESPVR defined as a parabolic relation with the

TABLE 1. Hemodynamics of four HFpEF phenotypes,[4] typical values for HFrEF patients[11] and reference values for healthy adults.[37]

	HFpEF[4]				HFrEF[11]	Reference
	I	II	III	IV	preLVAD	Healthy[37]
LVEF (%)	64	58	62	62	17.1	62
CO (L/min)	3.3	4.1	4.2	6.3	3.2	5.1
Mean AP (mmHg)	83	76	77	95	76.9	89
PCWP (mmHg)	21	19	23	25	28.3	9
Mean PAP (mmHg)	31	28	31	36	38.8	14
CVP/RAP (mmHg)	12	11	13	14	15.5	5
HR (bpm)	75	90	70	72	90.1	63
τ (ms)[25,38]	54	54	54	54	24	35

LVEF left ventricular ejection fraction, *CO* cardiac output, *PCWP* pulmonary capillary wedge pressure, *CVP* central venous pressure, *RAP* right atrial pressure, *HR* heart rate, τ time constant of early ventricular relaxation, *AP* arterial pressure, *PAP* pulmonary arterial pressure.

vertex at the coordinates (V_{sys}, P_{sys}) and crossing the volume axis of the pressure–volume plane at V_0[6]

$$ESPVR = \left[1 - \left(\frac{V_{sys} - V(t)}{V_{sys} - V_0}\right)\right] \times P_{sys}, \qquad (1)$$

with the units mL for volumes and mmHg for pressures. For the *EDPVR* we used the empirically found equation as presented in Klotz *et al.*[17]:

$$EDP = \alpha \times EDV^{\beta}, \qquad (2)$$

with α and β being dimensionless parameters and values for EDP are in mmHg and for EDV are in mL.

The active atria were adapted to have enlarged volumes and similar properties as proposed by Burkhoff *et al.*[4] The ventricular elastance curve was adjusted according to Moscato *et al.*[25] to mimic the typical elevated time constant during the early relaxation phase observed in HFpEF patients. To mimic the hydraulic properties of the cardiovascular system, the components of the arterial and venous system were modeled as 3- and 2-element Windkessel models[36] respectively. In Fig. 1, a schematic of the model, which was implemented in Matlab/Simulink (The MathWorks, Natick, MA, USA), is presented.

Numerical Model of the Valveless Pulsatile Device and Its Driving Unit

A simplified schematic of the proposed working principle is presented in Fig. 2. The pump consists of a pumping chamber, a cannula, a membrane, and a connection for the pneumatic drive. To investigate the effect of the pump in a cardiovascular system with different heart failure types, all these system components were incorporated in the numerical model. The pump chamber and its cannula were included in the form of a hydraulic resistance, inertance, and compliance ("Pump" in Fig. 1). The resistance mimicking the membrane was altered between a low value during filling and ejection and a high value once the end-positions, corresponding to a full or empty pump, were reached (Table 2). The pneumatic driveline and the air-filled pump chamber were modeled as a resistance and a varying compliance depending on the actual air volume in the system.

In a first step, the maximum stroke volume of the device was adjusted to 30 mL in order to model a pulsatile device with a size similar to the modern RBPs (e.g., HVAD or HeartMate 3). Second, the stroke volume was increased to 60 mL in order to examine the influence of the stroke volume on the hemodynamic outcomes. With a greater stroke volume, a greater achievable effect of such a pump would be expected.

The air compressor of the pneumatic driving unit ("Driving Unit" in Fig. 1) was implemented with a maximum flow rate (Q_{air_max}) of 133.3 mL/s for the 30 mL pump and 233.3 mL/s for the 60 mL pump. The compressor generated positive and negative pressures in two tanks with an air volume of 200 and 150 mL respectively. The pressures in these tanks (P_{pos}, P_{neg}) determined the compressors output (Q_{air}) defined by a simplified numerical model based on the following assumptions: the suction as well as the discharge characteristics were described by a pressure-flow relationship with a negative linear slope and steeper characteristics at the suction side [$k_{suc} = -0.1556$ mL/s $(\text{mmHg})^{-1}$ vs. $k_{dis} = -0.1333$ mL/s $(\text{mmHg})^{-1}$ in Eq. (3)]. This model represents typical pneumatic performance characteristics of commercially available micro diaphragm gas pumps[8]:

$$Q_{air} = Q_{air\_max} + \left(k_{dis}P_{pos} + k_{suc}P_{neg}\right), \qquad (3)$$

with the units mL/s for the air flow and mmHg for the relative pressure inputs.

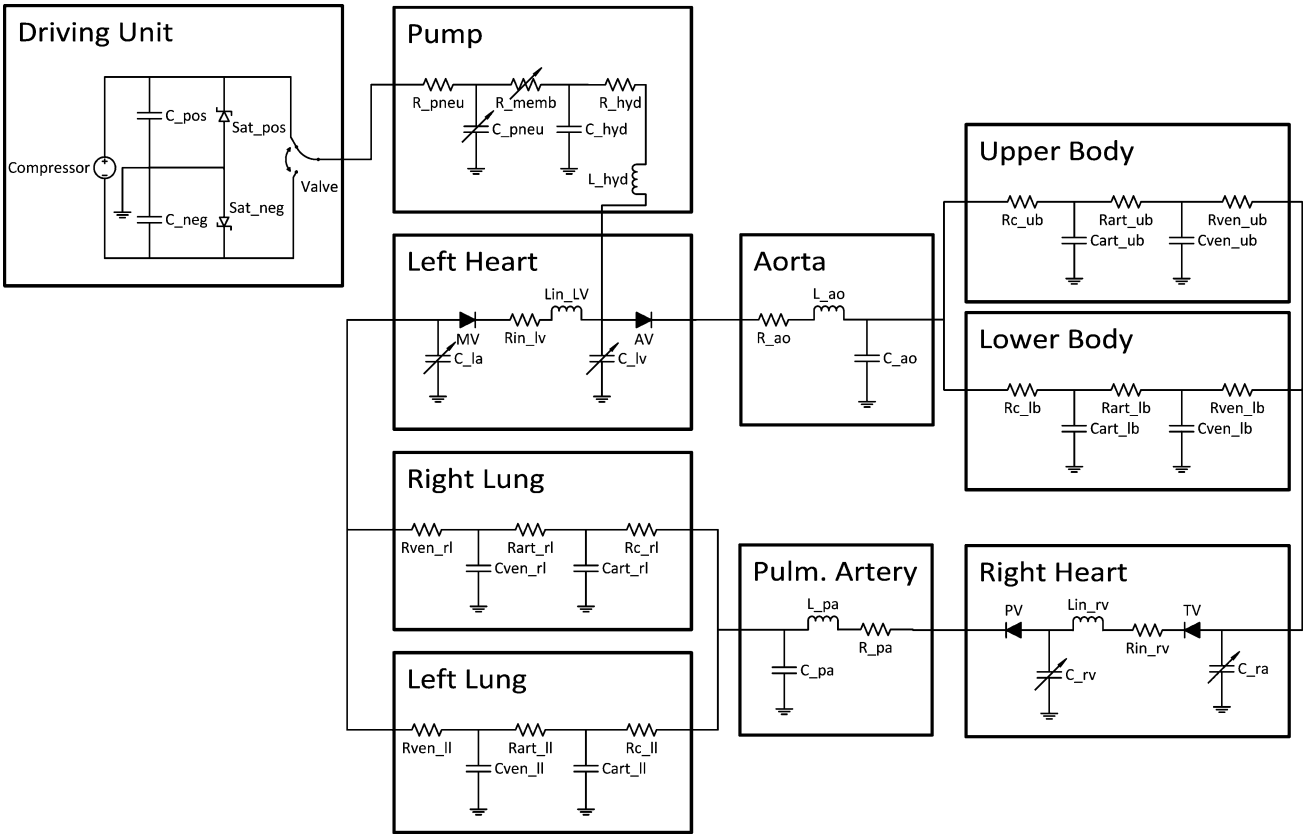

FIGURE 1. Electric analogue of the implemented numerical model including the valveless pump and the driving unit.

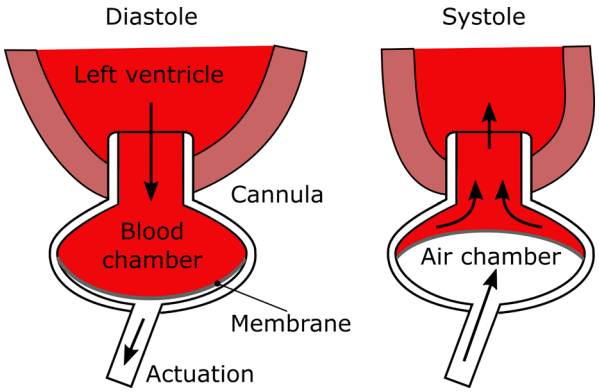

FIGURE 2. Exemplary schematic diagram of one possible embodiment of the pulsatile valveless device connected to the apex of the left ventricle.

The pressures in the tanks were limited by incorporated ideal pressure relief valves with saturations at 180/− 50 mmHg and 270/− 150 mmHg for the 30 and 60 mL pump respectively. An ideal switch ("valve" in Fig. 1) was triggered, connecting the pump to either the positive pressure plenum for pump ejection or the negative pressure plenum for pump filling during diastole. To optimize the functionality of the device, its ejection was initiated when the stiffness of the ventricle was high. This coincides with the time the aortic valve opens. Shortly after the maximum rise in the LVP was recorded (isovolumetric contraction phase), the ejection started, resulting in simultaneous ejection of the native LV and the assisting pump. The device filling began shortly after mitral valve opening.

Simulation Protocol

The numerical model was parameterized similarly to previously reported numerical models of the cardiovascular system[4,6,9,25,35] and adapted to achieve the hemodynamic conditions of the heart failure conditions presented in Table 1. The end-diastolic/end-systolic pressure volume relationships and the volumic state of the patient in terms of the mean circulatory filling pressure[24] without the device were iteratively adjusted to achieve the hemodynamics of each of the four HFpEF and the HFrEF groups within an accuracy of ± 7% at a given heart rate and arterial resistances derived from Table 1. For the ESPVR [Eq. (1)], the maximum achievable pressure during systole (P_{sys}) and the corresponding volume (V_{sys}) were adjusted to achieve the desired hemodynamics. For the EDPVR [Eq. (2)], the parameters α and β were adapted. Table 2 summarizes the model parameters for each of the investigated heart failure conditions.

TABLE 2. Values of parameters of the numerical model to achieve the typical hemodynamic condition presented in Table 1.

Parameter	Description	HFpEF I	HFpEF II	HFpEF III	HFpEF IV	HFrEF
R_ao	Resistance aorta ascend. (mmHg s/mL)	0.0075				
C_ao	Compliance aorta ascend. (mL/mmHg)	0.2356				
L_ao/L_pa	Inertance aorta ascend./pulm. artery (mmHg s^2/mL)	5.5669×10^{-5}				
Rc_ub/Rc_lb	Characteristic resistances upper/lower body (mmHg s/mL)	0.0427/0.0171	0.0308/0.0123	0.0295/0.0118	0.0246/0.0098	0.0378/0.0151
Cart_ub/Cart_lb	Arterial compliance upper/lower body (mL/mmHg)	0.236/0.71				
Rart_ub/Rart_lb	Arterial resistance upper/lower body (mmHg s/mL)	4.2305/1.6922	3.0534/1.2214	2.9254/1.1702	2.4305/0.9722	3.7465/1.4986
Cven_ub/Cven_lb	Venous compliance upper/lower body (mL/mmHg)	29.460/88.336				
Rven_ub/Rven_lb	Venous resistance upper/lower body (mmHg s/mL)	0.245/0.098				
R_pa	Resistance pulmonary artery (mmHg s/mL)	0.0075				
C_pa	Compliance pulmonary artery (mL/mmHg)	0.2356				
Rc_LL/Rc_RL	Characteristic resistances left/right lung (mmHg s/mL)	0.0034	0.0024	0.0021	0.0019	0.0037
Cart_LL/Cart_RL	Arterial compliance left/right lung (mL/mmHg)	1.145				
Rart_LL/Rart_RL	Arterial resistance left/right lung (mmHg s/mL)	0.3348	0.2425	0.2104	0.1929	0.3625
Cven_LL/Cven_RL	Venous compliance left/right lung (mL/mmHg)	9.07				
Rven_LL/Rven_RL	Venous resistance left/right lung (mmHg s/mL)	0.0255	0.0184	0.0160	0.0147	0.0276
Lin_rv/Lin_lv	Ventricular inflow inertances (mmHg s^2/mL)	3.1315×10^{-5}				
Rin_rv/Rin_lv	Ventricular inflow resistances (mmHg s/mL)	0.0038				
C_hyd	Hydraulic compliance (cannula and pump) (mL/mmHg)	0.0025				
R_hyd	Hydraulic resistance (cannula and pump) (mmHg s/mL)	Laminar ($Re \leq 2300$): 0.004 Turbulent ($Re > 2300$): $1.35 \times 10^{-4} \times \lvert Q \rvert$				
L_hyd	Hydraulic inertance (cannula and pump) (mmHg s^2/mL)	0.004				
R_pneu	Pneumatic resistance (Driveline and pump) (mmHg s/mL)	Laminar ($Re \leq 2300$): 0.0378 Turbulent ($Re > 2300$): $4.94 \times 10^{-4} \times \lvert Q \rvert$				
C_pneu	Pneumatic compliance (Driveline and pump) (mL/mmHg)	Pump filled: 0.0132 30 mL pump empty: 0.0528 60 mL pump empty: 0.0925				
C_pos	Compliance air reservoir pos. pressure (200 mL) (mL/mmHg)	0.264				
C_neg	Compliance air reservoir neg. pressure (150 mL) (mL/mmHg)	0.198				
R_memb	Resistance membrane (mmHg s/mL)	Moving: 0.010 End-positions: 12.0				
MCFP	Mean circulatory filling pressure (mmHg)	17	16.5	19	22	21
LV V_{sys}/P_{sys}	Vertex coordinates of the LV ESPVR (mL and mmHg)	125/230	130/180	135/210	150/220	205/70
LV α/β	LV EDPVR parameters	6.77×10^{-6}/3.52	9.19×10^{-6}/3.32	5.91×10^{-7}/3.88	2.04×10^{-9}/4.77	2.91×10^{-7}/3.41
RV V_{sys}/P_{sys}	Vertex coordinates of the RV ESPVR (mL and mmHg)	200/45	210/50	200/55	180/85	220/50
RV α/β	RV EDPVR parameters	3.26×10^{-6}/3.10				

Q flow rate in mL/s, *LV* left ventricle, *RV* right ventricle, *EDPVR* end-diastolic pressure volume relation, *ESPVR* end-systolic pressure volume relation, *Re* reynolds number.

Then, the pump was virtually connected to the ventricle and turned on. The resulting hemodynamics with the device (30 and 60 mL pump volume) and without the device were compared for all groups.

RESULTS

Figure 3 indicates typical simulated flow, volume and pressure waveforms with the 30 mL pump for the phenotype HFpEF I at a heart rate of 75 bpm for two cardiac cycles. Simulated pressures of the pneumatic as well as the hydraulic part of the pump and within the left ventricle are depicted. From the pump volume in the lower panel, it can be derived that the pump is driven in co-pulsation to the heart, ejecting during peak systole (pump volume decreases to 0 mL) and filling during diastole until a pump volume of 30 mL is reached. During ejection/filling of the pump, the pressure in the pneumatic system (blue, upper panel) slightly drops/increases since air is quickly released from/added to the tanks. Once the pump is filled/emptied, the compressor restores the maximum/minimum pressure conditions in the pneumatic system. The pump pressure (red, upper panel) is strongly influenced by the dynamic properties of the blood containing parts of the pump system as well as the membrane, leading to a pressure overshoot when ejection/filling of the device is started and transient oscillations as soon as the membrane reaches its end-positions.

Key parameters investigated to quantify the effects of MCS on HFpEF and HFrEF hemodynamic states were the mean arterial pressure (MAP), mean left atrial pressure (LAP), cardiac output (CO), and mean pulmonary artery pressure (PAP). As soon as the simulation reached a steady state, these parameters were recorded at a sampling rate of 100 Hz and averaged over 10 s. Figure 4 illustrates the key hemodynamic findings of the simulation study.

Cardiac Output and Arterial Pressure

In unassisted conditions, the simulations show that the CO in HFpEF I-III and HFrEF phenotypes is reduced compared to healthy subjects.[1] It can be derived from Fig. 4 that support with the 30 mL valveless pump increases the CO in all HFpEF phenotypes by at least 0.8 L/min. In contrast, in the HFrEF condition, the CO improves only slightly by 0.3 L/min. In all conditions, a device stroke volume of 60 mL nearly doubles the observed increases in CO.

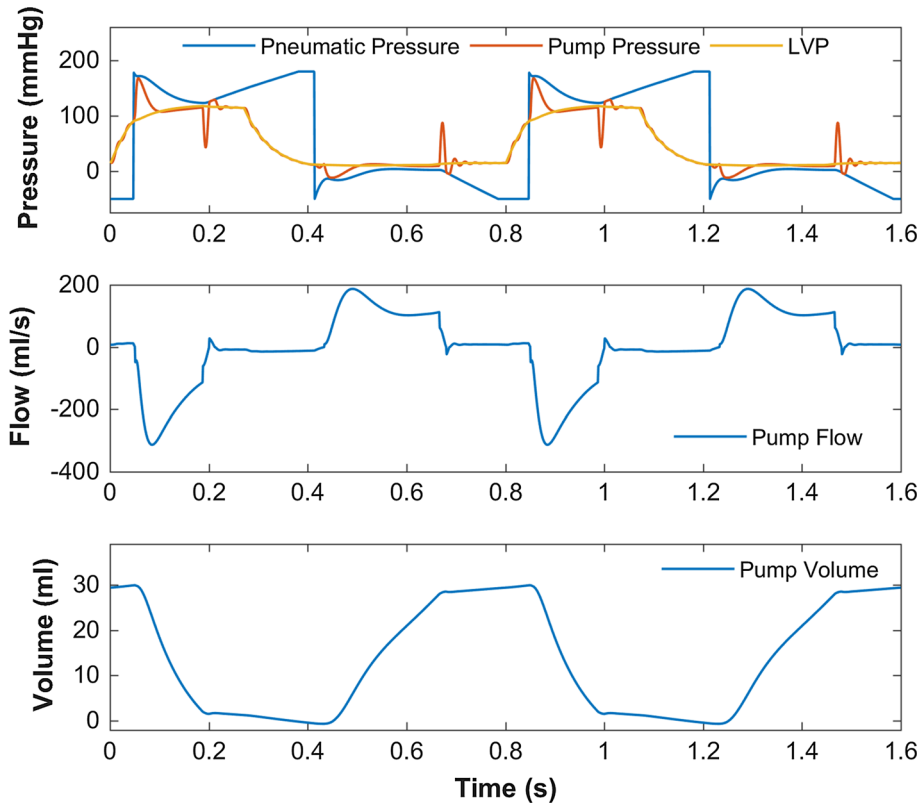

FIGURE 3. Pressures (upper panel), pump flow (middle panel) and pump volume (lower panel) for the 30 mL valveless pump in the HFpEF I phenotype during two cardiac cycles.

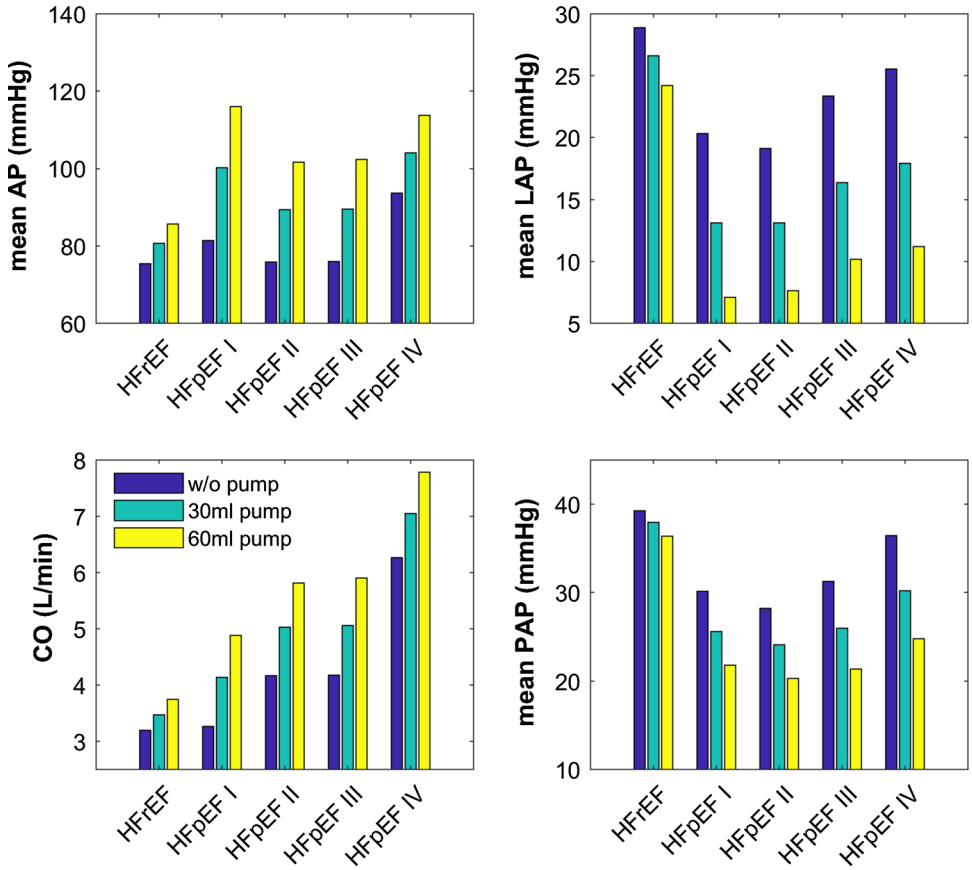

FIGURE 4. Hemodynamic parameters without (blue) and with the pump with two different volumes [30 (green) and 60 (yellow) mL].

Mechanical support with a 30 mL pump raises the MAP in all HFpEF groups by 11% (HFpEF IV) to 23% (HFpEF I); the same with a 60 mL pump was 22% (HFpEF IV) to 43% (HFpEF I). In the HFrEF condition, the proposed device leads to a less substantial increase in MAP by 7% and 14% with the 30 and 60 mL pump respectively.

Left Atrial and Pulmonary Pressures

When unassisted, all simulated heart failure conditions show a mean LAP above 19 mmHg, which indicates the necessity of left atrial and pulmonary decompression. In fact, for all HFpEF phenotypes, the 30 mL pump decompresses the left atrium by at least 30%, whereas this effect is less pronounced (reduction by 8%) in the HFrEF condition. This effect is amplified by use of a 60 mL pump assist: reduction in LAP by more than 56% in the HFpEF conditions and a drop of 16% in HFrEF condition are revealed.

For the HFpEF phenotypes, the mean PAP decreases by at least 15% with the 30 mL pump and more than 28% with the 60 ml pump. The effect of the device is again less pronounced in the HFrEF condition with a drop in PAP of 4 and 7% respectively.

Pressure–Volume Relationships of the Left Ventricle

Figure 5 depicts the pressure–volume (PV) loops, the ESPVRs as well as the EDPVRs (dashed lines) of the left ventricle for the five investigated groups in unassisted and in a 30 mL pump assisted case. It is notable that the end-diastolic and end-systolic volumes in HFrEF and HFpEF states differ substantially, with a much flatter ESPVR and EDPVR in the HFrEF condition.

Additionally, differences between the HFpEF phenotypes are evident: the HFpEF I group indicates the steepest ESPVR, whereas the ESPVR is similar in the three other phenotypes. The EDPVR is steepest in HFpEF I patients, followed by HFpEF III, indicating a stiff ventricle and a small ventricular cavity. The HFpEF IV phenotype reaches the largest ventricular volume in end-diastole, almost similar to that in a healthy heart.

Supported by the proposed co-pulsation device, the end-diastolic volume of the left ventricle in all heart

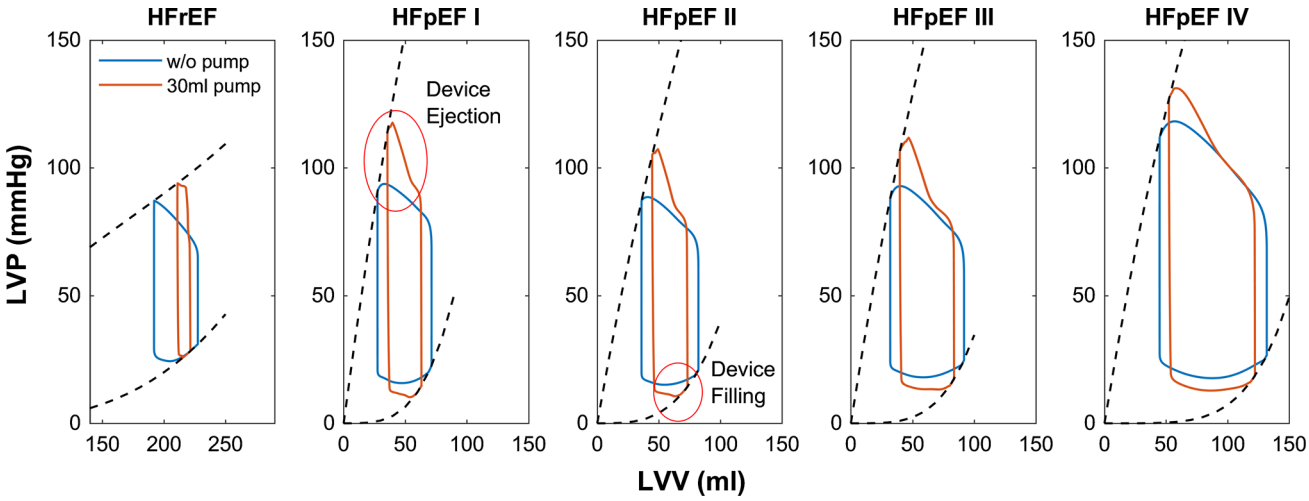

FIGURE 5. PV Loops of the five investigated groups without (blue) and with the 30 mL pump (red). ESPVRs and EDPVRs are indicated by dashed lines.

failure conditions is reduced in comparison to the unsupported state. In all HFpEF phenotypes, the end-systolic volumes are only slightly affected, whereas the end-systolic pressures are markedly increased. In contrast, the end-systolic volume in the HFrEF condition is elevated and the end-systolic pressure only slightly affected. It can be observed that the ejection of the device during systole results in a general decrease in left ventricular volume and increase in pressure in the HFpEF phenotypes (red circle in Fig. 5, panel 2) due to the stiff properties of the myocardium. In the HFrEF condition, however, the myocardium is less stiff and hence, the ventricular volume remains almost constant during the device ejection phase.

Shortly after mitral valve opening, the filling phase of the device starts, leading to a decrease in ventricular volume (red circle shown in Fig. 5, panel 3, indicates device filling).

Pressure–Volume Relationships of the Left Ventricle and the Pump

In order to precisely analyze the modus operandi of the co-pulsation device, the combined PV loops of the left ventricle and the device were investigated for the HFrEF and the HFpEF I condition (Fig. 6). The inherent working principle of the device can be observed: during diastole the pump lowers the ventricular diastolic pressures and during systole it ejects in co-pulsation with the ventricle thereby increasing the ventricular pressure.

It becomes evident that the amount of ejected blood through the aortic valve is strongly related to the stiffness of the ventricle during systole and thus the steepness of the ESPVR. The changes in total stroke volume are less pronounced in the HFrEF situation since both the end-diastolic and the end-systolic volumes increase in tandem with the device volume, thus shifting the entire PV loop to the right. In contrast, the end-diastolic volume in the HFpEF case rises with only a slight elevation in end-systolic volume, thus translating into increased stroke volume and improved hemodynamics.

DISCUSSION

In this simulation study, a novel MCS treatment option tailored to HFpEF patients with predominantly diastolic dysfunction was propounded and investigated. This device constitutes a valveless volume displacement support pump. A similar device was already introduced by Landesberg *et al.*[19,20] for the support of HFrEF patients, but has not yet been investigated for the use in HFpEF patients. Compared to hemodynamic reference values (Table 1), this pulsatile pump connected to the ventricle and driven in co-pulsation improves hemodynamics only marginally in end-stage HFrEF patients, whereas it enhances and potentially normalizes hemodynamics in selected HFpEF phenotypes. The device is opportunely suited for patients with a small ventricular cavity and stiff diastolic and systolic properties. The stiffer the ESPVR, the larger the volume ejected by the device through the left ventricle during systole. The efficiency of the device, as defined by the augmented stroke volume per device volume, is around 30–45% in HFpEF patients, while it is only about 10% in HFrEF patients. In the latter, most of the device ejection is being absorbed by the compliance of the dilated left ventricle.

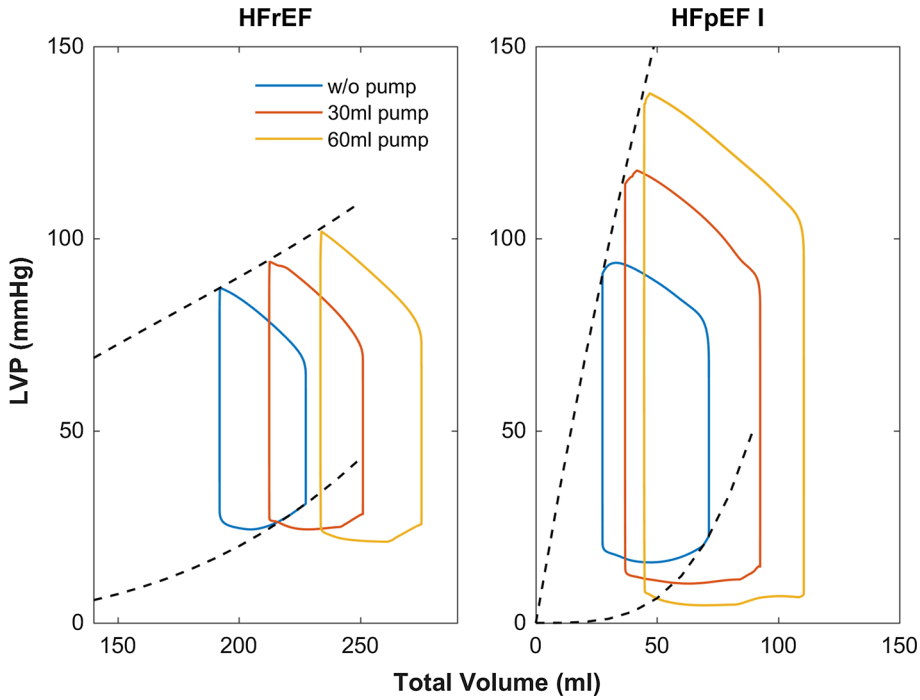

FIGURE 6. PV Loops of the ventricle and the pump for the HFrEF case (left) and the HFpEF I case (right) using 30 and 60 mL device stroke volumes.

It is predicted that the HFpEF I group may benefit the most from the use of such a device, followed by groups III and II. The HFpEF IV group may also benefit from such an assist device by achieving an increase in CO and decrease in LAP. However, due to the pathologic volume status in these patients, probably induced by renal impairment, it remains debatable whether increasing the CO in an already hypertensive arterial state with the proposed system or a RBP[4] is a favorable treatment option.

Two devices with 30 and 60 mL stroke volumes were investigated. The 30 mL pump could be designed to the size of a state-of-the-art RBP (e.g., Heartware VAD, Medtronic Inc., HeartMate3, Abbott Inc.). If successful, it may be implanted less invasively (such as a lateral thoracotomy).[12] Additionally, due to the single inlet and outlet cannula there is no need for an outlet graft anastomosis. The 60 mL pump was investigated to analyze the upper potential limit of the working principle of the system. A similar technology with a 30 mL stroke volume placed in a pacemaker-like pocket has been introduced in the clinical arena as a counter-pulsation device (Symphony, Abiomed Inc, Massachusetts, USA).[5] In contrast to the suggested device, the Symphony system with subclavian cannulation was used to reduce afterload during systole and increase myocardial perfusion during diastole, which was hypothesized to improve hemodynamics in case of HFrEF.

RBPs pump blood continuously during the heart cycle and are intrinsically at a greater risk of severe suction episodes in cases of small ventricular cavities. The proposed co-pulsation device addresses this risk of suction episodes through an increased end-systolic ventricular volume (Fig. 5) and its potential for device filling with slight negative pressures in the pump chamber only (Fig. 3).

It must be noted that such a system acts in co-pulsation to the heart. Hence, it's highly dependent on the synchronization with the cardiac systole, posing a challenge in patients with significant arrhythmogenicity. Further studies using appropriate models will be needed to investigate the functionality and the filling mechanism of the device in arrhythmic patients.

In spite of the efficacy of RBPs, patients suffer from several adverse events related to the compromised hemocompatibility of these devices,[34] leading to von Willebrand factor deficiency,[7] platelet activation and apoptosis,[32] hemolysis,[2] and resulting in major bleedings, cerebral strokes, and pump thrombosis.[18,28] Although the shear rate in contemporary clinical pulsatile devices is lower, the valve regions are susceptible to thrombosis due to the long residence times around the valve discs or leaflets.[13] The proposed pulsatile device does not need valves, thus eliminating the risk prone component. Nevertheless, short residence times of the blood within the device are crucial design considerations to prevent potential thrombus formation. Inno-

vative flow path design in the similar Symphony device proved to reduce persistent blood stagnation and flow separation without any thrombus formation in animal experiments.[10] This indicates the technical feasibility of a hemocompatible design of such a system.

Limitations

This study is subjected to the usual limitations of simulation studies. No baroreflex function or long-term adaptation mechanisms were implemented due to the scarcity of clinical data for the different HFpEF phenotypes. The hydraulic and pneumatic models of the pump system were carefully developed based on physical principles regarding resistances, inertances and compliances. A physical model of the pump and its driving unit is not yet available; therefore, the model idealizes several aspects such as an isothermic behavior, valves, tubes and other components. Such a model serves the aim of this study to achieve a proof-of-concept for the hemodynamic efficacy of the pump system, which was successfully realized previously using numerical models for similar purposes.[4,25] *In-vivo* studies are required to support the results of this study; however, in a conceptual manner, such simulation studies are meaningful to investigate the interaction between the cardiovascular system and MCS.

The heterogeneity of the HFpEF patient population and insufficiently understood mechanisms behind HFpEF encumber modeling of the disease in its entire complexity. This study followed the previously proposed HFpEF phenotype classification of Burkhoff *et al.*,[4] covering the most important subgroups of HFpEF patients with well-defined hemodynamics.

CONCLUSION

In this simulation study, a valveless co-pulsation device connected to the left ventricle with a single cannula and a small pump size demonstrated its potential to improve hemodynamics in HFpEF patients with diastolic dysfunction.

ACKNOWLEDGMENTS

This work is part of the Zurich Heart project under the umbrella of ''University Medicine Zurich''.

FUNDING

This study was funded by the UZH Foundation.

CONFLICT OF INTEREST

Marcus Granegger, Hitendu Dave, Walter Knirsch, Bente Thamsen, Martin Schweiger and Michael Hübler declare that they have no conflict of interest.

ETHICAL APPROVAL

This article does not contain any studies with human participants or animals performed by any of the authors.

REFERENCES

[1]Agostoni, P., C. Vignati, P. Gentile, *et al*. Reference values for peak exercise cardiac output in healthy individuals. *Chest*. 151:1329–1337, 2017.

[2]Birschmann, I., M. Dittrich, T. Eller, *et al*. Ambient hemolysis and activation of coagulation is different between HeartMate II and HeartWare left ventricular assist devices. *J. Heart Lung Transpl*. 33:80–87, 2014.

[3]Borlaug, B. A. Heart failure with preserved ejection fraction. In: Management of heart failure2nd, Vol. 1, edited by R. Baliga, and G. Haas. New York: Springer, 2010, pp. 216–219.

[4]Burkhoff, D., M. S. Maurer, S. M. Joseph, *et al*. Left atrial decompression pump for severe heart failure with preserved ejection fraction: theoretical and clinical considerations. *JACC Heart Fail*. 3:275–282, 2015.

[5]Cecere, R., R. D. Dowling, and N. Giannetti. Initial clinical experience with the symphony heart assist system. *Ann. Thorac. Surg*. 99:298–301, 2015.

[6]Colacino, F. M., F. Moscato, F. Piedimonte, *et al*. Left ventricle load impedance control by apical VAD can help heart recovery and patient perfusion: a numerical study. *ASAIO J*. 53:263–277, 2007.

[7]Crow, S., C. Milano, L. Joyce, *et al*. Comparative analysis of von willebrand factor profiles in pulsatile and continuous left ventricular assist device recipients. *ASAIO J*. 56:441–445, 2010.

[8]Diaphragm Gas Pumps—KNF. https://www.knf.com/products/oem-pumps/product/categories/diaphragm-gas-pumps/micro-pumps/. Accessed 30 Nov 2018.

[9]Fresiello, L., B. Meyns, A. Di Molfetta, and G. Ferrari. A model of the cardiorespiratory response to aerobic exercise in healthy and heart failure conditions. *Front. Physiol*. 7:189, 2016.

[10]Giridharan, G. A., C. Lederer, A. Berthe, *et al*. Flow dynamics of a novel counterpulsation device characterized by CFD and PIV modeling. *Med. Eng. Phys*. 33:1193–1202, 2011.

[11]Gupta, S., K. Woldendorp, K. Muthiah, *et al*. Normalisation of haemodynamics in patients with end-stage heart failure with continuous-flow left ventricular assist device therapy. *Heart Lung Circ*. 23:963–969, 2014.

[12]Haberl, T., J. Riebandt, S. Mahr, *et al*. Viennese approach to minimize the invasiveness of ventricular assist device implantation. *Eur. J. Cardio-thorac. Surg*. 46:991–996, 2014.

[13]Hetzer, R., F. Kaufmann, and E. M. D. Walter. Paediatric mechanical circulatory support with berlin heart EXCOR:

development and outcome of a 23-year experience. *Eur. J. Cardio-thorac. Surg.* 50:203–210, 2016.
[14]Kasner, M., D. Sinning, J. Lober, *et al.* Heterogeneous responses of systolic and diastolic left ventricular function to exercise in patients with heart failure and preserved ejection fraction. *ESC Heart Fail.* 2:121–132, 2015.
[15]Katz, D. H., L. Beussink, A. J. Sauer, *et al.* Prevalence, clinical characteristics, and outcomes associated with eccentric versus concentric left ventricular hypertrophy in heart failure with preserved ejection fraction. *Am. J. Cardiol.* 112:1158–1164, 2013.
[16]Kirklin, J. K., F. D. Pagani, R. L. Kormos, *et al.* Eighth annual INTERMACS report: special focus on framing the impact of adverse events. *J. Heart Lung Transpl.* 36:1080–1086, 2017.
[17]Klotz, S., M. L. Dickstein, and D. Burkhoff. A computational method of prediction of the end-diastolic pressure-volume relationship by single beat. *Nat. Protoc.* 2:2152–2158, 2007.
[18]Krabatsch, T., I. Netuka, J. D. Schmitto, *et al.* Heartmate 3 fully magnetically levitated left ventricular assist device for the treatment of advanced heart failure-1 year results from the Ce mark trial. *J. Cardiothorac. Surg.* 12:23, 2017.
[19]Landesberg, A., E. Konyukhov, R. Shofti, *et al.* Augmentation of dilated failing left ventricular stroke work by a physiological cardiac assist device. *Ann. N. Y. Acad. Sci.* 1015:379–390, 2004.
[20]Landesberg, A., A. Shenhav, R. Shofty, *et al.* Effects of synchronized cardiac assist device on cardiac energetics. *Ann. N. Y. Acad. Sci.* 1080:466–478, 2006.
[21]Li, J., P. M. Becher, S. Blankenberg, and D. Westermann. Current treatment of heart failure with preserved ejection fraction: should we add life to the remaining years or add years to the remaining life? *Cardiol. Res. Pract.* 1:1–9, 2013.
[22]Loor, G., and G. Gonzalez-Stawinski. Pulsatile vs. continuous flow in ventricular assist device therapy. *Best Pract. Res. Clin. Anaesthesiol.* 26:105–115, 2012.
[23]Lund, L. H., J. Matthews, and K. Aaronson. Patient selection for left ventricular assist devices. *Eur. J. Heart Fail.* 12:434–443, 2010.
[24]Magder, S. Volume and its relationship to cardiac output and venous return. *Crit. Care.* 20:271, 2016.
[25]Moscato, F., C. Wirrmann, M. Granegger, *et al.* Use of continuous flow ventricular assist devices in patients with heart failure and a normal ejection fraction: a computer-simulation study. *J. Thorac. Cardiovasc. Surg.* 145:1352–1358, 2013.
[26]Muthiah, K., J. Phan, D. Robson, *et al.* Centrifugal continuous-flow left ventricular assist device in patients with hypertrophic cardiomyopathy. *ASAIO J.* 59:183–187, 2013.
[27]Penicka, M., J. Bartunek, H. Trakalova, *et al.* Heart failure with preserved ejection fraction in outpatients with unexplained dyspnea. A pressure-volume loop analysis. *J. Am. Coll. Cardiol.* 55:1701–1710, 2010.
[28]Rogers, J. G., F. D. Pagani, A. J. Tatooles, *et al.* Intrapericardial left ventricular assist device for advanced heart failure. *N. Engl. J. Med.* 376:451–460, 2017.
[29]Shah, A. M., B. Claggett, N. K. Sweitzer, *et al.* Prognostic importance of impaired systolic function in heart failure with preserved ejection fraction and the impact of spironolactone. *Circulation* 132:402–414, 2015.
[30]Sharma, K., and D. A. Kass. Heart failure with preserved ejection fraction: mechanisms, clinical features, and therapies. *Circ. Res.* 115:79–96, 2014.
[31]Slaughter, M. S., J. G. Rogers, C. A. Milano, *et al.* Advanced heart failure treated with continuous-flow left ventricular assist device. *N. Engl. J. Med.* 361:2241–2251, 2009.
[32]Slaughter, M. S., M. A. Sobieski, J. D. Graham, *et al.* Platelet activation in heart failure patients supported by the heartmate ii ventricular assist device. *Int. J. Artif. Organs* 34:461–468, 2011.
[33]Topilsky, Y., N. L. Pereira, D. K. Shah, *et al.* Left ventricular assist device therapy in patients with restrictive and hypertrophic cardiomyopathy. *Circ. Heart Fail.* 4:266–275, 2011.
[34]Uriel, N., P. C. Colombo, J. C. Cleveland, *et al.* Hemocompatibility-related outcomes in the MOMENTUM 3 trial at 6 months: a randomized controlled study of a fully magnetically levitated pump in advanced heart failure. *Circulation* 135:2003–2012, 2017.
[35]Ursino, M. Interaction between carotid baroregulation and the pulsating heart: a mathematical model. *Am. J. Physiol.* 275:H1733–H1747, 1998.
[36]Westerhof, N., J. W. Lankhaar, and B. E. Westerhof. The arterial windkessel. *Med. Biol. Eng. Comput.* 47:131–141, 2009.
[37]Wolsk, E., R. Bakkestrøm, J. H. Thomsen, *et al.* The influence of age on hemodynamic parameters during rest and exercise in healthy individuals. *JACC Heart Fail.* 5:337–346, 2017.
[38]Zile, M. R., C. F. Baicu, and W. H. Gaasch. Diastolic heart failure—abnormalities in active relaxation and passive stiffness of the left ventricle. *N. Engl. J. Med.* 19:1953–1959, 2004.